Pamukkale Univ Muh Bilim Derg, 29(3), 274-280, 2023

Pamukkale Üniversitesi Mühendislik Bilimleri Dergisi

Pamukkale University Journal of Engineering Sciences

Free vibration analysis of elastically restrained cantilever Timoshenko beam with attachments

Ucunda ekleme bulunan elastik mesnetli konsol Timoshenko kirişin serbest titreşim analizi

Yasar PALA[1*], *Caglar KAHYA*[1]

[1]Department of Mechanical Engineering, Engineering Faculty, Bursa Uludağ University, Bursa, Turkey.
mypala@uludag.edu.tr, ckahya@uludag.edu.tr

Received/Geliş Tarihi: 10.01.2022 Revision/Düzeltme Tarihi: 30.06.2022 doi: 10.5505/pajes.2022.93467
Accepted/Kabul Tarihi: 27.07.2022 Research Article/Araştırma Makalesi

Abstract

This paper investigates the lateral vibration of a cantilever Timoshenko beam with attachments. It is assumed that the beam carries a mass attached to the free end with a linear spring and there exists a rotational spring at the left end. Depending upon these assumptions, mode shapes and natural frequencies are obtained in terms of non-dimensional parameters which describe the effects of additional mass, linear spring and rotational spring. The results are tabulated, and the comparison of Timoshenko and Euler-Bernoulli beam approaches are carried out for some parameters. Results reveal that natural frequencies decrease while the values of end mass increase. Large values of the rotational spring constant cause high natural frequencies.

Keywords: Timoshenko beam, Vibration, Spring-mass system, Natural frequencies, Mode shapes.

Öz

Bu çalışmada ucunda eklemeler olan bir konsol Timoshenko kirişin titreşim analizi yapılmıştır. Kirişin, serbest ucunda lineer yay ile bağlanmış kütle taşıdığı ve sol ucunda dönme yayı bulunduğu varsayılmıştır. Bu kabullere göre doğal frekanslar ve mod şekilleri, kütlenin, serbest uca bağlı lineer yayın ve dönme yayının etkilerini tanımlayan boyutsuz parametreler cinsinden elde edilmiştir. Sonuçlar tablolaştırılmış ve bazı parametreler için Timoshenko ve Euler-Bernoulli kiriş yaklaşımlarının karşılaştırılması yapılmıştır. Sonuçlar göstermiştir ki doğal frekanslar uç kütlesinin artması ile düşmektedir. Burulma yayı sabitinin büyük değerleri, yüksek doğal frekansları ortaya çıkartmaktadır.

Anahtar kelimeler: Timoshenko kiriş, Titreşim, kütle-yay sistemi, Doğal frekanslar, Mod şekilleri.

1 Introduction

Many authors have studied the free and forced vibration of Euler-Bernoulli beams under various boundary conditions. Low [1] studied the vibration of a beam carrying several masses on the beam at different locations, but he did not include spring attachment. However, for the cases where the rotary and shear effects must be considered, Timoshenko beam theory must be utilized. Several authors have investigated the free and forced vibration of Timoshenko beam with attachments under various boundary conditions. Majkut [2] proposed a method to obtain a single equation for both free and forced vibration of the Timoshenko beams. Several papers are also available on the free vibration of cantilever beams carrying a concentrated mass. Laura et al. [3], studied the free vibration of a clamped-free beam which carries a finite mass at the free end and obtained the natural frequencies and modal shapes. Chang [4] investigated the vibration characteristics of a simply supported beam with a heavy concentrated mass at its centre. Banerjee [5] investigated the free vibration of a beam carrying a spring-mass system using the dynamic stiffness method. He obtained the natural frequencies and the first five mode shapes. Rossit and Laura investigated the lateral vibration of a beam with a mass attached to the end with a linear spring. Relatively simpler Bernoulli beam theory has been utilized in the analysis [6]. However, for a thick beam carrying a mass load such as an electric motor or engine, Timoshenko beam theory must be used [7]-[10].

In addition, when the mass load is too heavy, the assumption of semi-rigid root must also be made due to the elastic nature of the end. Some researchers have focused on a cantilever Timoshenko beam. Rossit and Laura [11] studied a cantilever Timoshenko beam with a spring-mass system attached to the free end. A cantilever Timoshenko beam with a tip mass at the free end and having rotational and translational springs has been studied by Abramovich and Hamburger [12]. Salarieh and Ghorashi [13] analysed the free vibration of a cantilever Timoshenko beam with rigid mass and compared with other beam theories. In the work by Jafari-Talookolaei and Abedi [14], a new method was presented to obtain the exact solution for the free vibration of a Timoshenko beam with different boundary conditions. The vibration analysis of a cantilever beam with an eccentric three dimensional object has been investigated by Kati and Gökdag [15]. There are also several research works on the tapered Timoshenko beams. Lateral vibration analysis of a Timoshenko beam of variable cross-section carrying several masses is carried out in [16]. In that study, differential quadrature element method (DQEM) is used and the changing of the frequencies of the beam is studied in terms of parameters of the mass. Cekus [17] studied the free vibration of a cantilever tapered Timoshenko beam by using Lagrange multiplier formalism. The governing equations for the Timoshenko beams with geometrical non-uniformity and material inhomogeneity along the beam axis have been simplified by a new method [18].

*Corresponding author/Yazışılan Yazar

In the present study, the vibration analysis of a cantilever beam carrying a tip mass using Timoshenko theory is investigated. The free end carries a mass attached to the beam by means of a linear spring while the left hand side is semi-rigid with a rotational spring. Natural frequencies and related mode shapes are determined in terms of non-dimensional parameters.

2 Analysis

2.1 Frequency Analysis

Let us consider a Timoshenko beam with a semi-rigid root (Figure 1). The mass M is attached to the free end of the beam by means of a spring of coefficient k_0. L is the length of the beam, k_R is the rotational rigidity. It is well known that the transversal motion of the beam is governed by the equations [19] as follows:

$$\rho A\frac{\partial^2 y}{\partial t^2}=kAG\left(\frac{\partial^2 y}{\partial x^2}-\frac{\partial \psi}{\partial x}\right) \quad 1(a)$$

$$\rho I\frac{\partial^2 \psi}{\partial t^2}=kAG\left(\frac{\partial y}{\partial x}-\psi\right)+EI\frac{\partial^2 \psi}{\partial x^2} \quad 1(b)$$

Here, I is the moment of inertia, E is the modulus of elasticity, G is the shear modulus of elasticity, A is the cross-sectional area, ρ is the density of the beam, k is the shape factor, y is the vertical displacement, ψ is the bending angle.

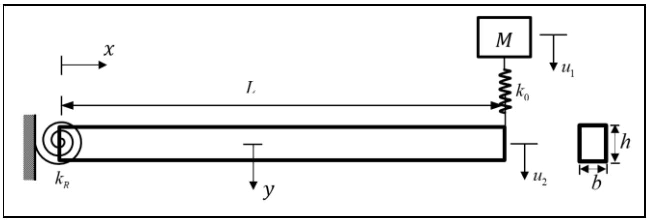

Figure 1. Timoshenko beam with various end conditions.

Eqs. 1(a), 1(b) must be solved together with the boundary conditions described. Assume that

$$y(x,t)=LY(x)\mathrm{e}^{i\omega t} \quad 2(a)$$

$$\psi(x,t)=\Psi(x)\mathrm{e}^{i\omega t} \quad 2(b)$$

Where, t is the time, ω is the angular frequency. Here, L is substituted for brevity. Substituting Eqs. (2) into Eq. (1), we have

$$Y''(\xi)+\lambda^2 s^2 Y(\xi)-\Psi'(\xi)=0 \quad 3(a)$$

$$s^2\Psi''(\xi)-[1-\lambda^2 r^2 s^2]\Psi(\xi)+Y'(\xi)=0 \quad 3(b)$$

Where;

$$s^2=\frac{EI}{kAGL^2}\ ,\ \lambda^2=\frac{\rho A\omega^2 L^4}{EI}\ ,\ \xi=\frac{x}{L}\ ,\ r^2=\frac{I}{AL^2} \quad (4)$$

By eliminating $\Psi(\xi)$ and its derivatives in Eqs. (3), it can be combined into a single equation as follows:

$$Y^{iv}(\xi)+PY''(\xi)+QY(\xi)=0 \quad (5)$$

Where;

$$P=\frac{\rho\omega^2L^2}{E}\left(1+\frac{E}{kG}\right)\ ,\ Q=\frac{\rho\omega^2L^2}{E}\left(\frac{\rho\omega^2L^2}{kG}-\frac{AL^2}{I}\right) \quad (6)$$

In order to solve Eq. (5), we assume $Y(\xi)=\mathrm{e}^{\alpha\xi}$. The characteristic equation and its roots are obtained as

$$\alpha^4+P\alpha^2+Q=0$$

$$\alpha_1=-i\beta_1\ ,\ \alpha_2=i\beta_1,\ \alpha_3=-\beta_2,\ \alpha_4=\beta_2 \quad (7)$$

Here,

$$\beta_1=\sqrt{\frac{P+\sqrt{\Delta}}{2}}\ ,\ \beta_2=\sqrt{\frac{-P+\sqrt{\Delta}}{2}},\ \Delta=P^2-4Q \quad (8)$$

The solution of Eq. (5) can be written as

$$Y(\xi)=C_1\sin\beta_1\xi+C_2\cos\beta_1\xi+C_3\sinh\beta_2\xi+C_4\cosh\beta_2\xi$$

We now utilize the first of Eqs.(3) to obtain $\Psi(\xi)$. Inserting $Y(\xi)$ into the first of Eqs.(3) yields

$$\Psi'(\xi)=\bar{m}_1C_1\sin\beta_1\xi+C_2\bar{m}_1\cos\beta_1\xi+C_3\bar{m}_2\sinh\beta_2\xi+C_4\bar{m}_2\cosh\beta_2\xi \quad (9)$$

Where;

$$\bar{m}_1=\lambda^2s^2-\beta_1^2\ ,\ \bar{m}_2=\lambda^2s^2+\beta_2^2 \quad (10)$$

Integrating Eq.(9) gives

$$\Psi(\xi)=-m_1C_1\cos\beta_1\xi+m_1C_2\sin\beta_1\xi+m_2C_3\cosh\beta_2\xi+m_2C_4\sinh\beta_2\xi \quad (11)$$

Where;

$$m_1=\frac{\bar{m}_1}{\beta_1}\ ,\ m_2=\frac{\bar{m}_2}{\beta_2} \quad (12)$$

After Eq. (9) is integrated, a constant value would surely appear in Eq. (11). However, by substituting the solution forms obtained into Eqs. (1), it is quite simple to show that it is indeed zero. The coefficients C_1, C_2, C_3, C_4 must be determined by using the boundary conditions at both ends of the beam. These boundary conditions can be written as follows:

At $\xi=0$:

$$Y(\xi)|_{\xi=0}=0 \quad 13(a)$$

$$\frac{EI}{L}\Psi'(\xi)\Big|_{\xi=0}=k_R\Psi(\xi)|_{\xi=0} \quad 13(b)$$

At $\xi=1$:

$$\Psi'(\xi)|_{\xi=1}=0 \quad 13(c)$$

$$Y'(\xi)|_{\xi=1}-\Psi(\xi)|_{\xi=1}=-\frac{F}{kAG}\mathrm{e}^{-i\omega t} \quad 13(d)$$

Here, F is the force exerted on the beam by the spring at $\xi=1$. In order to find the force F, we write the equation of motion for the mass M:

$$M\frac{d^2u_1}{dt^2}=k_0(u_2(1,t)-u_1(1,t)) \quad (14)$$

Here, u_1 is the displacement of the mass, and u_2 is the deflection of the end. Let us assume $u_2-u_1=u$. Inserting this form into Eq. (14) gives

$$M\frac{d^2u_2}{dt^2} = M\frac{d^2u}{dt^2} + k_0u \tag{15}$$

Let us now assume the following solution forms for u_2 and u:

$$u_2 = LY(1)e^{i\omega t} \quad 16(a)$$

$$u = LNe^{i\omega t} \quad 16(b)$$

Substituting these forms into Eq. (15), we obtain

$$N = \frac{MY(1)\omega^2}{M\omega^2 - k_0} \quad , \quad u = \frac{MY(1)\omega^2 L}{M\omega^2 - k_0}e^{i\omega t} \tag{17}$$

The force F acted upon by the spring now reads

$$F = k_0 u = \left(\frac{M\omega^2 L}{\frac{M\omega^2}{k_0} - 1}\right)Y(1)e^{i\omega t} \tag{18}$$

By combining Eq.(13d) and Eq. (18), the last form of the last condition in Eqs.(13) can be rewritten as

$$Y'(\xi)|_{\xi=1} - \Psi(\xi)|_{\xi=1} = a_3Y(1) \tag{19}$$

Where;

$$a_3 = \frac{-M\omega^2 L}{kAG\left(\frac{M\omega^2}{k_0} - 1\right)} \tag{20}$$

By utilizing the boundary conditions, the four equations are obtained in terms of the unknown coefficients as follows:

$$C_2 + C_4 = 0 \quad 21(a)$$

$$\overline{m}_1C_2 + \overline{m}_2C_4 + m_1b_1C_1 - m_2b_1C_3 = 0 \quad 21(b)$$

$$d_1C_1 + d_2C_2 + d_3C_3 + d_4C_4 = 0 \quad 21(c)$$

$$e_1C_1 + e_2C_2 + e_3C_3 + e_4C_4 = 0 \quad 21(d)$$

Where;

$$\begin{gathered} b_1 = \frac{k_R L}{EI} \\ d_1 = \overline{m}_1\sin\beta_1 \quad , \quad d_2 = \overline{m}_1\cos\beta_1 \\ d_3 = \overline{m}_2\sinh\beta_2 \quad , \quad d_4 = \overline{m}_2\cosh\beta_2 \\ e_1 = \beta_1\cos\beta_1 + m_1\cos\beta_1 - a_3\sin\beta_1 \\ e_2 = -\beta_1\sin\beta_1 - m_1\sin\beta_1 - a_3\cos\beta_1 \\ e_3 = \beta_2\cosh\beta_2 - m_2\cosh\beta_2 - a_3\sinh\beta_2 \\ e_4 = \beta_2\sinh\beta_2 - m_2\sinh\beta_2 - a_3\cosh\beta_2 \end{gathered} \tag{22}$$

Eqs. (21) can also be written in matrix form as

$$[A][C] = [0] \tag{23}$$

Where;

$$[A] = \begin{bmatrix} 0 & 1 & 0 & 1 \\ m_1b_1 & \overline{m}_1 & -m_2b_1 & \overline{m}_2 \\ d_1 & d_2 & d_3 & d_4 \\ e_1 & e_2 & e_3 & e_4 \end{bmatrix} \quad , \quad [C] = \begin{bmatrix} C_1 \\ C_2 \\ C_3 \\ C_4 \end{bmatrix} \tag{24}$$

The frequency equation is obtained by taking $\det[A] = 0$. The explicit form of the frequency equation is as follows:

$$\begin{aligned} -m_1b_1(d_3e_4 - d_4e_3) - m_2b_1(d_1e_4 - d_4e_1) \\ - \overline{m}_2(d_1e_3 - d_3e_1) \\ - m_1b_1(d_2e_3 - d_3e_2) \\ + \overline{m}_1(d_1e_3 - d_3e_1) \\ + m_2b_1(d_1e_2 - d_2e_1) = 0 \end{aligned} \tag{25}$$

In the case of a rigid wall, by taking $b_1 = \infty$, Eq.(25) can be simplified into the form

$$\begin{aligned} -m_1(d_3e_4 - d_4e_3) - m_2(d_1e_4 - d_4e_1) \\ - m_1(d_2e_3 - d_3e_2) \\ + m_2(d_1e_2 - d_2e_1) = 0 \end{aligned} \tag{26}$$

2.2 Eigen-Function analysis

Eigen-functions of the problem can be determined by writing the coefficients C_2, C_3, C_4 in terms of C_1:

$$C_2 = -s_1C_1 \quad 27(a)$$

$$C_3 = s_2C_1 \quad 27(b)$$

$$C_4 = s_1C_1 \quad 27(c)$$

Thus, $Y(\xi)$ is obtained in the form of

$$Y(\xi) = C_1[\sin\beta_1\xi - s_1\cos\beta_1\xi + s_2\sinh\beta_2\xi + s_1\cosh\beta_2\xi] \tag{28}$$

Where;

$$\begin{gathered} s_1 = \frac{h_1}{h_2} \quad , \quad s_2 = \frac{m_1}{m_2} - \frac{(\overline{m}_1 - \overline{m}_2)}{m_2b_1}\left(\frac{h_1}{h_2}\right) \\ h_1 = d_1 + \frac{m_1}{m_2}d_3 \quad , \quad h_2 = d_2 + d_3\frac{(\overline{m}_1 - \overline{m}_2)}{m_2b_1} - d_4 \end{gathered} \tag{29}$$

To find the value of C_1, the condition of orthogonality can be utilized:

$$\begin{aligned} \int_0^1 (\rho AL^2Y_n(\xi)Y_m(\xi) + \rho I\Psi_n(\xi)\Psi_m(\xi))d\xi \\ + \frac{MLk_0^2}{(M\omega_m^2 - k_0)(M\omega_n^2 - k_0)}Y_n(1)Y_m(1) = \delta_{nm} \end{aligned} \tag{30}$$

Here, δ_{nm} is Kronecker delta. Inserting Eqs. (27) into Eq. (30) and evaluating the integral, the constant C_1 can be obtained.

3 Results and discussion

In order to validate the present solution, a cantilever Timoshenko beam with carrying mass-spring system at the free end is considered by taking $b_1 = 10^{12}$, whose equation is given in Eqs. (22). The reason why b_1 is taken high is that the rotational spring's effect becomes inactive and therefore behaves as a fixed support. The results are compared with the study of Rossit and Laura [11] in Table 1, and it is seen that they are in good agreement. After validation study, numerical studies have been carried out for different combinations of dimensionless variables. They are tabulated in Tables 2-7. The beam properties used in the analysis are $E = 210$ GPa, $G = 80.76$ GPa, $k = 5/6$, $\rho = 7800$ kg/m^3, $L = 1$ m, $h = 0.1$ m, $b = 0.05$m.

For ease of interpretation, dimensionless parameters a_4 and a_5 are defined as follows:

$$a_4 = \rho AL/M \quad \text{and} \quad a_5 = k_0L^3/EI$$

Here, a_4 is the ratio of the beam mass to the added mass and a_5 is the ratio of the linear spring coefficient to the bending stiffness.

The variation of natural frequencies with b_1 are shown in Tables 2, 3. In Table 3, the mass is assumed to be zero. It can be seen from these tables that, for increasing values of b_1, which is associated with the rotational spring coefficient (k_R), all natural frequencies increase. The frequency values obtained for zero mass are higher than those found for the case of non-zero mass (Table 2). Thus, the mass attached decreases the values of frequencies. In addition, for the beam with a non-zero end mass, the rates of increase in each natural frequency are slightly higher than those for the case with no mass, except for the first mode.

Table 1. Dimensionless frequencies (Ω) of the beam with spring mass at its free end. ($r_G = \sqrt{I/A}$ and $\Omega = \sqrt{\omega^2 L^4 \rho A/EI}$).

	Ω_1	Ω_2	Ω_3	Ω_4	Ω_5	Ω_6	
$a_5 = 0.1$, $a_4 = 5$, $r_G/L = 0.01$	0.695154	3.571296	21.89797	60.74417	117.5177	191.1809	Present
	0.695153	3.5713	21.898	60.7442	117.518	191.181	[11]
$a_5 = 1$, $a_4 = 2$, $r_G/L = 0.01$	1.205223	4.101427	21.98027	60.77323	117.5324	191.1898	Present
	1.20522	4.10143	21.9803	60.7732	117.532	191.19	[11]
$a_5 = 10$, $a_4 = 1$, $r_G/L = 0.01$	1.418757	7.440483	22.85213	61.06872	117.6808	191.2786	Present
	1.41875	7.44048	22.8521	61.0687	117.681	191.279	[11]
$a_5 = \infty$, $a_4 = 0.5$, $r_G/L = 0.01$	1.157604	15.78384	49.79175	102.1493	171.7104	257.062	Present
	1.15760	15.7838	49.7918	102.149	171.710	257.062	[11]
$a_5 = 0.1$, $a_4 = 5$, $r_G/L = 0.05$	0.694873	3.493776	19.11237	46.60619	78.90373	113.7507	Present
	0.694873	3.49378	19.1124	46.6062	78.9037	113.751	[11]
$a_5 = 1$, $a_4 = 2$, $r_G/L = 0.05$	1.200783	4.02287	19.19198	46.6337	78.9174	113.7587	Present
	1.20078	4.02287	19.192	46.6337	78.9174	113.759	[11]
$a_5 = 10$, $a_4 = 1$, $r_G/L = 0.05$	1.403972	7.291428	20.05012	46.91589	79.05583	113.8392	Present
	1.40397	7.29143	20.0501	46.9159	79.0558	113.839	[11]
$a_5 = \infty$, $a_4 = 0.5$, $r_G/L = 0.05$	1.143655	14.23311	39.46071	70.84078	105.3227	141.3791	Present
	1.14365	14.2331	39.4607	70.8408	105.323	141.379	[11]

Table 2. The variation of frequencies with b_1 for $a_4 = 0.1, a_5 = 1$.

b_1	ω_1 (rad/s)	ω_2 (rad/s)	ω_3 (rad/s)	ω_4 (rad/s)	ω_5 (rad/s)
0.1	13.88	273.72	2283.63	6948.23	13504.55
0.4	23.97	306.44	2320.06	6983.90	13534.9
0.8	29.28	340.31	2364.28	7028.73	13573.58
1	30.84	354.28	2384.72	7050.06	13592.19
10	39.48	526.79	2799.79	7585.85	14114.64
100	40.8	591.87	3092.27	8125.24	14778.07

Table 3. The variation of frequencies with b_1 for $a_4 = 10^{10}$ ($M \cong 0$), $a_5 = 1$.

b_1	ω_1 (rad/s)	ω_2 (rad/s)	ω_3 (rad/s)	ω_4 (rad/s)	ω_5 (rad/s)
0.1	80.98	2264.48	6942.44	13501.84	21336.22
0.4	156.55	2301.38	6978.16	13532.19	21361.5
0.8	212.27	2346.12	7023.05	13570.89	21393.92
1	232.66	2366.79	7044.4	13589.51	21409.61
10	441.86	2785.06	7580.75	14112.12	21874.97
100	512.47	3078.68	8120.5	14775.7	22555.41

In Table 4, the values of a_5, which equals to k_0L^3/EI, is increased and natural frequencies are tabulated. It is observed that natural frequencies increase with increasing values of a_5. This is valid for all frequencies. However, at frequencies with high modes, the values are not appreciably affected by the varying values of a_5. It can also be concluded from Table 4 that the frequencies do not change too much for large values of a_5. This means that the spring becomes ineffective and behaves like a massless rigid body.

Table 4. The variation of frequencies with a_5 for $a_4 = 0.5$, $b_1 = 0.1$.

a_5	ω_1 (rad/s)	ω_2 (rad/s)	ω_3 (rad/s)	ω_4 (rad/s)	ω_5 (rad/s)
0.01	10.08	85.11	2264.67	6942.49	13501.87
0.05	19.04	100.67	2265.43	6942.72	13501.97
0.1	22.98	117.9	2266.38	6943.01	13502.11
0.5	28.52	211.66	2274.03	6945.33	13503.19
1	29.48	288.18	2283.67	6948.23	13504.55
10	30.41	808.53	2467.5	7001.6	13529.22
100	30.51	1408.2	3953.76	7632.74	13799.03
1000	30.52	1521.75	5447.79	10900.82	16906.39
20000	30.52	1533.89	5625.76	11741.15	19243.49
25000	30.52	1534.01	5627.55	11748.61	19262.59

The variation of frequencies with a_4 involving mass M is shown in Table 5. As expected, the frequencies increase with increasing a_4. However, unlike the frequencies with low modes, the frequencies with high modes are not influenced by the change of a_4.

Table 5. The variation of frequencies with a_4 for $a_5 = 0.1$, $b_1 = 0.1$.

a_4	ω_1 (rad/s)	ω_2 (rad/s)	ω_3 (rad/s)	ω_4 (rad/s)	ω_5 (rad/s)
0.01	3.32	115.41	2266.38	6943.01	13502.11
0.05	7.41	115.61	2266.38	6943.01	13502.11
0.1	10.46	115.86	2266.38	6943.01	13502.11
0.5	22.98	117.9	2266.38	6943.01	13502.11
1	31.78	120.57	2266.38	6943.01	13502.11
10	68.87	175.95	2266.39	6943.01	13502.11
10000	80.96	2263.92	4737.62	6943.52	13502.15

In Table 6, in the case of nearly rigid wall ($k_R \gg 0$), frequencies are obtained for varying values of a_5. The increase in k_0 (or a_5) values has a higher effect on the frequencies with low modes than the higher ones.

Table 6. The variation of frequencies with a_5 for $a_4 = 0.5$, $b_1 = 10^{10}$ ($k_R \cong \infty$).

a_5	ω_1 (rad /s)	ω_2 (rad/s)	ω_3 (rad/s)	ω_4 (rad/s)	ω_5 (rad/s)
0.01	10.57	523.36	3131.69	8236.47	14940.56
0.05	23.49	526.75	3132.22	8236.66	14940.66
0.1	32.94	530.97	3132.89	8236.9	14940.77
0.5	69.21	563.93	3138.26	8238.77	14941.71
1	91.29	603.12	3145.01	8241.12	14942.88
10	154.93	1071.19	3273.06	8284.15	14964.17

Tables 7(a), 7(b) show the difference between Timoshenko and Euler-Bernoulli beam approaches. In the case of rigid wall, the results for Euler-Bernoulli beam are taken from the literature [6]. The difference between these results becomes smaller at lower modes. In Table 7(b), the constant b_1 has been taken as $b_1 = 10^{12}$, while it is $b_1 = 10^{10}$ in the Table 7(a). It is shown that $b_1 = 10^{10}$ is the value that can be considered as a rigid wall since the changes of frequencies become negligible. From the comparison of both tables, it can be concluded that the difference between the results of both models is not due to the rotational spring's coefficient (k_R), but due to the shear and rotary effects of the beam.

Table 7(a). Comparison of Timoshenko and Euler-Bernoulli beams for $a_4 = 1$, $a_5 = 1$, $b_1 = 10^{10}$ ($k_R \cong \infty$), $h/L = 0.1$ $\left(\beta^4 = \frac{\rho A}{EI}\omega^2 L^4\right)$.

	β_1	β_2	β_3	β_4	β_5
Timoshenko Beam	0.92653	2.0106	4.5822	7.4175	9.9881
Euler Beam	0.92705	2.0177	4.7038	7.8568	10.996
Difference	0.056%	0.353 %	2.619 %	5.752 %	9.606 %

Table 7(b). Comparison of Timoshenko and Euler-Bernoulli beams for $a_4 = 1$, $a_5 = 1$, $b_1 = 10^{12}$ ($k_R \cong \infty$), $h/L = 0.1$ $\left(\beta^4 = \frac{\rho A}{EI}\omega^2 L^4\right)$.

	β_1	β_2	β_3	β_4	β_5
Timoshenko Beam	0.92653	2.0106	4.5822	7.4175	9.9881
Euler Beam	0.92705	2.0177	4.7038	7.8568	10.996
Difference	0.056%	0.353 %	2.619 %	5.752 %	9.606 %

Mode shapes are demonstrated in Figures 2-11. The first four ones are associated with the changing values of b_1 in the case that end mass exists. On the contrary of these mode shapes, end mass has been considered not existing by taking $a_4 = 10^{10}$ in Figures 6, 7. Figures 8-11 show how a_5 affects the mode shapes.

The first four Figures show that the increasing value of b_1 changes the linearity of the beginning part of the mode shapes, and peak points slightly move to the free end.

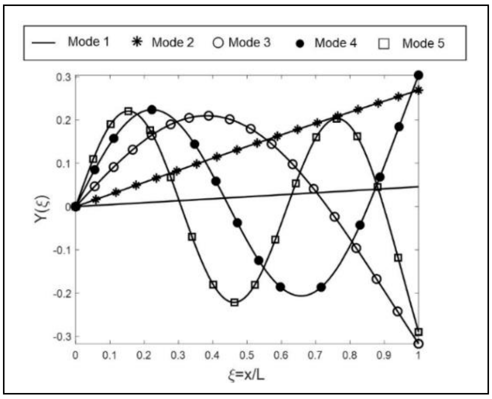

Figure 2. Mode shapes for $b_1 = 0.1$, $a_5 = 1$, $a_4 = 0.1$.

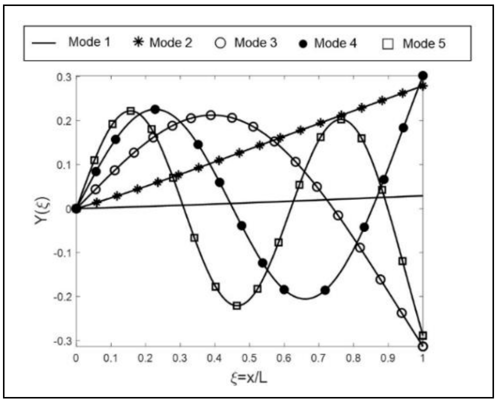

Figure 3. Mode shapes for $b_1 = 1$, $a_5 = 1$, $a_4 = 0.1$.

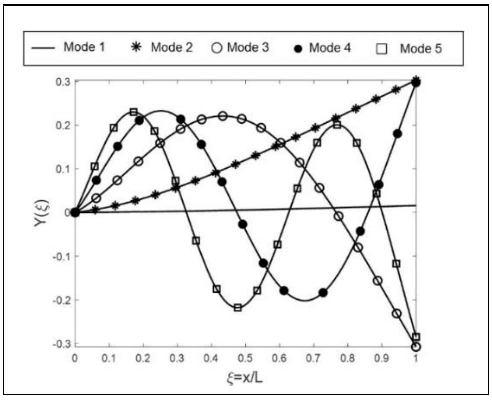

Figure 4. Mode shapes for $b_1 = 10,\ a_5 = 1,\ a_4 = 0.1$.

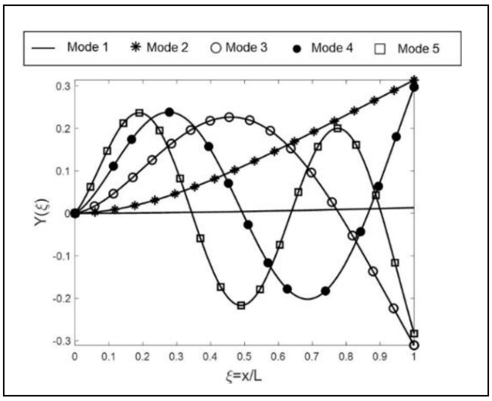

Figure 5. Mode shapes for $b_1 = 100,\ a_5 = 1,\ a_4 = 0.1$.

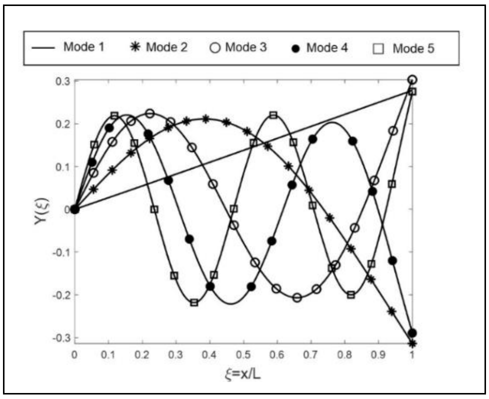

Figure 6. Mode shapes for $b_1 = 0.1, a_5 = 1, a_4 = 10^{10}$ $(M \cong 0)$.

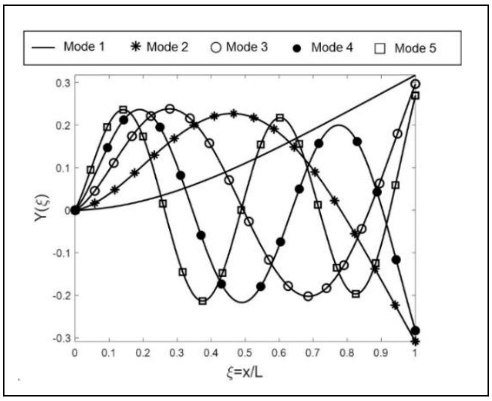

Figure 7. Mode shapes for $b_1 = 100,\ a_5 = 1,$ $a_4 = 10^{10}$ $(M \cong 0)$.

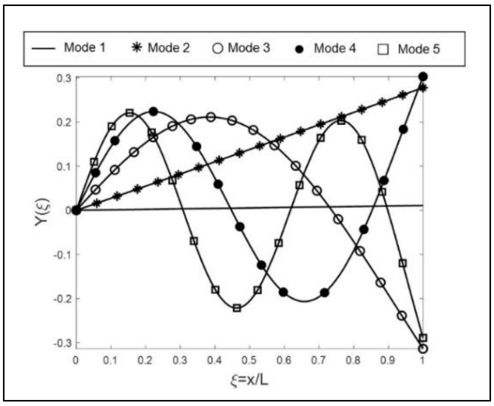

Figure 8. Mode shapes for $b_1 = 0.1,\ a_5 = 0.01,\ a_4 = 0.5$.

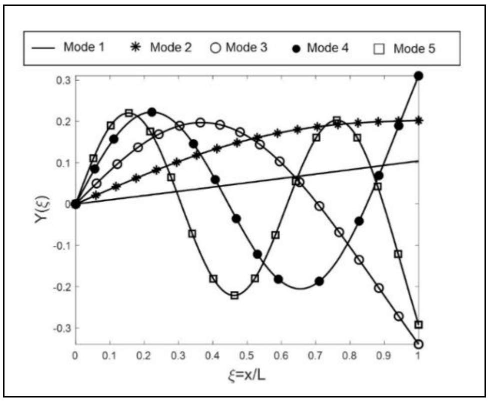

Figure 9. Mode shapes for $b_1 = 0.1,\ a_5 = 10,\ a_4 = 0.5$.

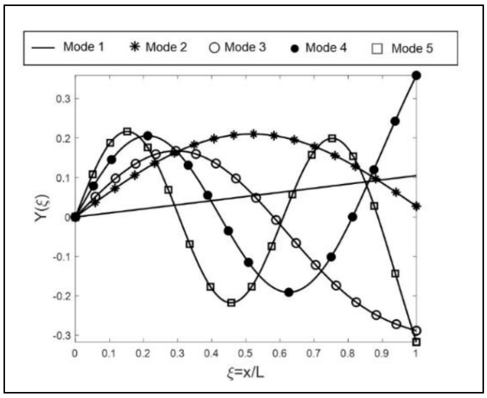

Figure 10. Mode shapes for $b_1 = 0.1,\ a_5 = 100,\ a_4 = 0.5$.

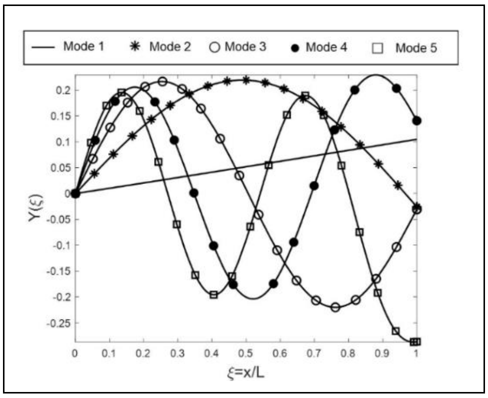

Figure 11. Mode shapes for $b_1 = 0.1,\ a_5 = 1000,\ a_4 = 0.5$.

It can be seen from Figures 6, 7 that if the end mass is assumed to be zero, the linearity of the initial part of the mode shapes is changed as in the case where the end mass exists. On the whole, it can be mentioned that mode shapes are slightly affected by the change of b_1 in this case. Moreover, Figures 2, 6 and Figures 5,7 show that the first mode shape is not observed in the case where the end mass does not exist. Namely, the nth mode shape in the case where there is no mass shows resemblance with the $(n+1)$th mode shape in the case where the end mass exists.

Figures 8-11 show that although mode shapes are more affected as the value of a_5 increases in terms of changing amplitudes and shapes, they are less affected in the first mode after the value of $a_5 = 10$.

4 Conclusion

In this study, mode shapes and natural frequencies were analysed in terms of some parameters such as a_4, a_5, b_1 for the elastically restrained cantilever Timoshenko beam carrying a spring mass system at its free end. Here, a_5 ($a_5 = k_0 L^3/EI$) and b_1 ($b_1 = k_R L/EI$) contain the ratios of linear spring and rotational spring coefficients to bending stiffness, respectively. a_4 ($a_4 = \rho AL/M$) is also the ratio of the beam mass to the added mass. The results have been tabulated in order to see the effects non-dimensional parameters on the frequencies. Mode shapes have also been obtained in terms of various values of parameters. In the general case, it has been seen that the increase in the end mass decreases the natural frequencies. Large values of a_5 (or k_0) increase the values of natural frequencies, except for the frequencies with high modes. Also, the natural frequency increases with increasing b_1 value. The frequency equation for extremely large values of b_1 has also been obtained. In order to see the effects of the parameters on the mode shapes, Figures 2-11 have been plotted. Except for the shape of the first mode, the other mode shapes are affected by the increment of a_5. Changing the value of b_1 also affects the mode shapes. Location of peak points and the shape of the initial parts are slightly influenced by b_1.

5 Author contribution statements

In the scope of this study, Yasar PALA in the formation of the idea, the formulation, the design and the literature review, the assessment of obtained results and writing; Caglar KAHYA in the formulation, numerical computations, writing, obtaining and examining the results.

6 Ethics committee approval and conflict of interest statement

There is no need to obtain permission from the ethics committee for the article prepared.

There is no conflict of interest with any person / institution in the article.

7 References

[1] Low KH. "On the methods to derive frequency equations of beams carrying multiple masses". *International Journal of Mechanical Sciences*, 43(3), 871-881, 2001.

[2] Majkut L. "Free and forced vibrations of Timoshenko beams described by single difference equation". *Journal of Theoretical and Applied Mechanics*, 47(1), 193-210, 2009.

[3] Laura PAA, Pombo JL, Susemihl EA. "A note on the vibrations of a clamped-free beam with a mass at the free end". *Journal of Sound and Vibration*, 37(2), 161-168, 1974.

[4] Chang CH. "Free vibration of a simply supported beam carrying a rigid mass at the middle". *Journal of Sound and Vibration*, 237(4), 733-744, 2000.

[5] Banerjee JR. "Free vibration of beams carrying spring-mass systems-a dynamic stiffness approach". *Computers and Structures*, 104-105, 21-26, 2012.

[6] Rossit CA, Laura PAA. "Free vibrations of a cantilever beam with a spring-mass system attached to the free end". *Ocean Engineering*, 28(7), 933-939, 2001.

[7] Stephen NG. "The second frequency spectrum of Timoshenko beams". *Journal of Sound and Vibration*, 80(4), 578-582, 1982.

[8] Dym CL, Shames IH. *Solid Mechanics, A Variational Approach*. Augmented ed. New York, USA, Springer, 2013.

[9] Zhu X, Li TY, Zhao Y, Liu JX. "Structural power flow analysis of Timoshenko beam with an open crack". *Journal of Sound and Vibration*, 297(1-2), 215-226, 2006.

[10] Yuan S, Ye K, Xiao C, Williams FW, Kennedy D. "Exact dynamic stiffness method for non-uniform Timoshenko beam vibrations and Bernoulli-Euler column buckling". *Journal of Sound and Vibration*, 303(3-5), 526-537, 2007.

[11] Rossit CA, Laura PAA. "Transverse, normal modes of vibration of a cantilever Timoshenko beam with a mass elastically mounted at the free end". *The Journal of the Acoustical Society of America*, 110(6), 2837-2840, 2001.

[12] Abramovich H, Hamburger O. "Vibration of a uniform cantilever Timoshenko beam with translational and rotational springs and with a tip mass". *Journal of Sound and Vibration*, 154(1), 67-80, 1992.

[13] Salarieh H, Ghorashi M. "Free vibration of Timoshenko beam with finite mass rigid tip load and flexural-torsional coupling". *International Journal of Mechanical Sciences*, 48(7), 763-779, 2006.

[14] Jafari-Talookolaei RA, Abedi M. "An exact solution for the free vibration analysis of Timoshenko beams". *Review of Applied Physics*, 3, 12-17, 2014.

[15] Kati HD, Gokdag H. "Vibration analysis of a Timoshenko beam carrying 3D tip mass by using differential transform method". *Structural Engineering and Mechanics*, 65(4), 381-388, 2018.

[16] Torabi K, Afshari H, Heidari-Rarani M. "Free vibration analysis of a non-uniform cantilever Timoshenko beam with multiple concentrated masses using DQEM". *Engineering Solid Mechanics*, 1(1), 9-20, 2013.

[17] Cekus D. "Free Vibration of a Cantilever Tapered Timoshenko Beam". *Scientific Research of the Institute of Mathematics and Computer Science*, 11(4), 11-17, 2012.

[18] Yuan J, Pao YH, Chen W. "Exact solutions for free vibrations of axially inhomogeneous Timoshenko beams with variable cross section". *Acta Mechanica*, 227, 2625-2643, 2016.

[19] Rao SS. *Mechanical Vibrations.* 5th ed. NJ, USA, Pearson Education Inc., 2011.